



ELSEVIER

28 February 2000

PHYSICS LETTERS A

Physics Letters A 266 (2000) 331–335

www.elsevier.nl/locate/physleta

Observation of dynamical localization in a rough microwave cavity

L. Sirko^{a,b,c}, Sz. Bauch^a, Y. Hlushchuk^a, P.M. Koch^b, R. Blümel^{d,*}, M. Barth^c,
U. Kuhl^c, H.-J. Stöckmann^c

^a Institute of Physics, Polish Academy of Sciences, Al. Lotników 32 / 46, 02-668 Warszawa, Poland

^b Department of Physics and Astronomy, State University of New York, Stony Brook, NY 11794-3800, USA

^c Fachbereich Physik, Universität Marburg, Renthof 5, D-35032 Marburg, Germany

^d Department of Physics, Wesleyan University, Middletown, CT 06459-0155, USA

Received 30 September 1999; accepted 18 January 2000

Communicated by A.R. Bishop

Abstract

We measure the angular momentum content of modes in a flat, near-circular microwave cavity with a rough perimeter and demonstrate localization in angular momentum space. Because Schrödinger's wave mechanics and Maxwell's electro-dynamics are equivalent for a 2d cavity, we compare our experimental results directly with the quantum theory of rough 2d cavities [K.M. Frahm and D.L. Shepelyansky, Phys. Rev. Lett. 78 (1997) 1440]. Introducing the concept of *effective roughness* we find good qualitative agreement. © 2000 Published by Elsevier Science B.V. All rights reserved.

PACS: 05.45.+b; 03.65.Sq; 72.15.Rn

The two most important mechanisms responsible for classical diffusion are disorder and chaos. Both mechanisms may lead to the localization of wavefunctions. The pinning of electron wavefunctions to sites of spatial disorder was first identified in a one-dimensional (1D) model by Anderson [1]. It is the dominant mechanism responsible for localization in solid state samples and is now universally known as *Anderson localization*. Disorder-induced localization in coordinate space is a ubiquitous phenomenon.

It has been observed, e.g., in microwave cavities with randomly placed obstacles [2], two-dimensional dielectric lattices [3], and a mixture of metallic and dielectric spheres [4]. A more subtle kind of localization, *dynamical localization*, may occur in classically chaotic systems. Here the disorder is not imposed on the system, but generated dynamically due to the chaotic features of the system [5–8].

2D chaotic billiards were proposed recently as fruitful systems for the study of dynamical localization [9]. At the interface between disorder and chaos are rough billiards, e.g. weakly deformed circular billiards introduced by Frahm and Shepelyansky [10,11]. It is this circular billiard perturbed by a rough boundary that this Letter addresses. We report

* Corresponding author. Tel. +1-860-6852032; fax: +1-860-685-2031.

E-mail address: rblumel@wesleyan.edu (R. Blümel).

the first experimental observation of dynamical localization in a rough billiard. Rough billiards are of considerable interest elsewhere, for example, in the context of microdisk lasers [12,13], ballistic electron transport in microstructures [14], and localization in discontinuous quantum systems [15].

We begin by recalling the localization theory presented in [10] for rough 2D billiards. Consider a billiard that is circular on average but with a rough boundary characterized by the radius function

$$R(\theta) = \langle R \rangle + \Delta R(\theta), \quad (1)$$

where $\langle R \rangle$ is the angular average of $R(\theta)$ and $|\Delta R(\theta)| \ll \langle R \rangle$. The function

$$\kappa(\theta) = \frac{1}{\langle R \rangle} \frac{dR(\theta)}{d\theta} \quad (2)$$

characterizes the roughness, and

$$\tilde{\kappa} = [\langle \kappa^2(\theta) \rangle]^{1/2} = \left[\frac{1}{2\pi} \int_0^{2\pi} \kappa(\theta)^2 d\theta \right]^{1/2} \quad (3)$$

is the roughness parameter. We may expand any wavefunction in the billiard as

$$\Psi(r, \theta) = \sum_{\ell=-\infty}^{\infty} a_{\ell} J_{\ell}(kr) \exp(i\ell\theta), \quad (4)$$

where the J_{ℓ} are Bessel functions of the first kind and $k = 2\pi/\lambda$ is the wavenumber. Although the sum in Eq. (4) extends over all angular momenta ℓ , for $\tilde{\kappa}$ small enough there is an angular momentum cutoff for $|\ell|$ at $\ell_{\max} \approx k\langle R \rangle$. This is a semiclassical estimate for the maximum possible angular momentum for a given k . Partial waves with angular momentum $|\ell| > \ell_{\max}$ correspond to evanescent waves and can be neglected. A rough billiard boundary breaks the rotational symmetry and leads to angular momentum diffusion. In this case, and under certain additional conditions to be discussed below, a range of wavefunctions in a rough billiard is exponentially localized in angular momentum space according to

$$|a_{\ell}| \sim \exp(-|\ell - \ell_0|/L), \quad (5)$$

where ℓ_0 is the localization center, i.e., the most probable value for ℓ , and L is the localization length.

Now we introduce a crucial new element, the *effective roughness*, into the localization theory of

rough billiards. At finite wavelength a cavity mode cannot resolve details of the perimeter on a scale much smaller than λ . Finite resolution at finite wavelength is an important concept throughout physics; it features prominently, e.g., in the theory of fractal billiards [16,17], a topic closely related to the rough billiards considered in this Letter. The limited resolving power of a cavity mode is due to its finite angular momentum content ($|\ell| \lesssim \ell_{\max}$).

Expanding $\Delta R(\theta)$ in a Fourier series

$$\Delta R(\theta) = \sum_{m=1}^{\infty} [A_m \cos(m\theta) + B_m \sin(m\theta)], \quad (6)$$

with real coefficients A_m and B_m , we define an *effective roughness parameter*

$$\tilde{\kappa}_{\text{eff}}^2 = \frac{1}{2\langle R \rangle^2} \sum_{m=1}^{\ell_{\max}} m^2 (A_m^2 + B_m^2). \quad (7)$$

The theory of dynamical localization predicts that the localization length L of the states in (5) is given by [10]

$$L = D, \quad (8)$$

where D is the classical diffusion constant. In quasilinear approximation D is obtained from the *rough map* defined in [10]. We obtain

$$L = 4(\ell_{\max}^2 - \ell_r^2) \tilde{\kappa}_{\text{eff}}^2, \quad (9)$$

where ℓ_r is the resonance angular momentum for the classical ray-tracing mapping of the rough billiard. Note that this is essentially Frahm and Shepelyansky's estimate [10] for L with the *bare roughness* $\tilde{\kappa}$ ($\ell_{\max} = \infty$ in (7)) replaced by the effective roughness $\tilde{\kappa}_{\text{eff}}$.

Depending on the value of L there are three qualitatively different dynamical regimes: (i) the perturbatively localized regime ($L \approx 1$), (ii) the dynamical localization regime ($1 < L < \ell_{\max}$), and (iii) the delocalized (ergodic) regime ($L > \ell_{\max}$). The existence of an exponentially localized regime was confirmed numerically in [10].

We now turn to our experimental demonstration of dynamical localization in a rough microwave cavity and the comparison of our results with the quantum theory of localization outlined above. To do so we exploit the known equivalence in 2D of Schrödinger's wave mechanics and Maxwell's electrodynamics for a flat cavity [18].

We used an aluminum cavity in the shape of a right cylinder. It had a mean radius $\langle R \rangle = 17.10 \pm 0.05$ cm, height $h = 0.77 \pm 0.01$ cm, area $A = 919 \pm 5$ cm², and perimeter $P = 110.3 \pm 0.3$ cm. We measured its radius function $R(\theta)$ with a digitizing tablet, obtaining a set of 753 data points (R_j, θ_j) with a radial resolution ΔR_j of about 0.1 mm. Fig. 1 shows the digitized normalized radius function $R_j/\langle R \rangle$. We excited the cavity at frequencies below the onset of the 3D electromagnetic mode at $f_{\text{cut}} = c/(2h) = 19.47 \pm 0.25$ GHz, where c is the speed of light. Therefore, all our experiments were performed for conditions guaranteeing the equivalence between quantum mechanics and electrodynamics.

We used the method described in [19] to measure the (electric field) wavefunction $\Psi(r, \theta)$ inside the cavity at 1 degree steps around a circle of fixed radius $r_0 = 16$ cm $< \langle R \rangle$. We used a vector network analyzer (Wiltron 360B) with two antennas ‘1’ and ‘2’ coupled to the cavity to measure the powers and relative phases needed to determine the four S-matrix elements of a two-port network. Measurement of the matrix element S_{11} for reflection from ‘1’ gave a quantity proportional to $|\Psi(r_0, \theta)|^2$ at the position of ‘1’. Measurement of the transmission matrix element S_{21} from ‘1’ to ‘2’ determined the sign of $\Psi(r_0, \theta)$. Fig. 2 shows the measured θ -dependence of the amplitude of two different wavefunctions $\Psi(r_0, \theta)$.

We extracted the amplitudes a_ℓ in Eq. (4) from the measurements as follows. Since the Bessel functions $J_\ell(x)$ become exponentially small for $\ell > x$, r_0 should be as large as possible; that is why we chose $r_0 = 16$ cm. We determined $a_\ell J_\ell(kr_0)$, and, consequently, a_ℓ , from a Fourier analysis of the $\Psi(r_0, \theta)$ data. Using standard techniques of error

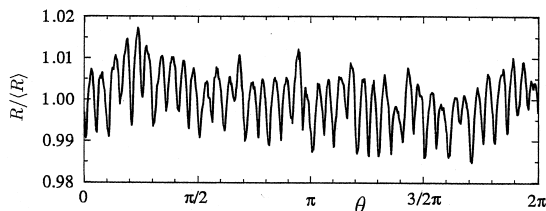


Fig. 1. Normalized radius function $R(\theta)/\langle R \rangle$ for the rough cavity used in our experiments.

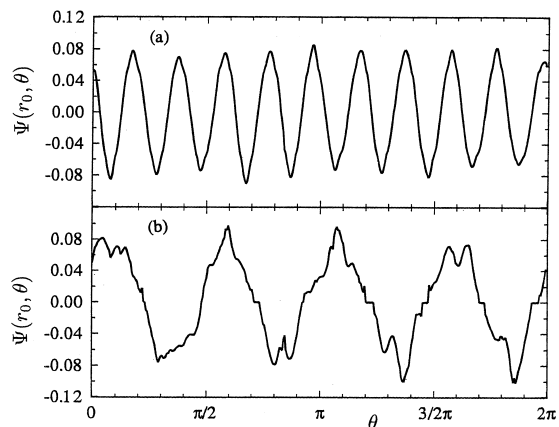


Fig. 2. Wavefunctions $\Psi(r_0 = 16 \text{ cm}, \theta)$ (in arbitrary units) for the modes at (a) 6.153 GHz and (b) 8.455 GHz.

propagation we determined the errors in a_ℓ from the uncertainties in the electric field measurements.

Fig. 3 shows semilogarithmically over the range $0 \leq \ell \leq kr_0$ the expansion coefficients a_ℓ and corresponding error bars for the two exponentially localized modes, respectively (a) 6.153 and (b) 8.455 GHz, used for Fig. 2. Because the electric field in (4) is a real-valued function, we have $a_{-\ell} = a_\ell^*$. Therefore Fig. 3 shows $|a_\ell|$ for $\ell \geq 0$ only. We used a weighted, linear, least-squares fit to each data set, i.e., exponential decay, to obtain the localization lengths. For case (a) we fitted the two wings of the

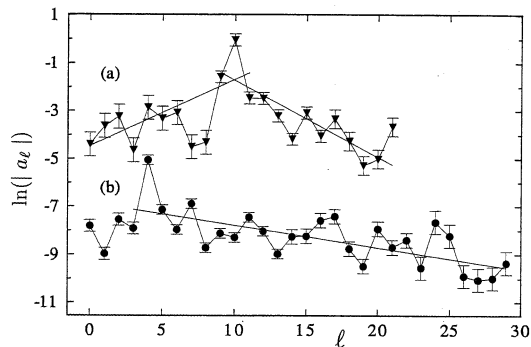


Fig. 3. Angular momentum content of two exponentially localized modes, (a) 6.153 GHz and (b) 8.455 GHz, respectively (the same as in Fig. 2). A weighted linear, least-squares fit (exponential decay) to each data set was made over the domain of ℓ covered by each fitted line; see the text. For clarity, graph (b) is shifted down by 4.

state independently and obtained $L \approx 4$ for both wings. Fitting only the right-hand wing of (b) we obtained $L \approx 10$.

Only (a) has the triangular shape expected from Eq. (5), since only for (a) is ℓ_0 large enough to separate the peak located at $\ell = \ell_0$ from its time-reversed twin at $\ell = -\ell_0$. The maximal angular momentum is $\ell_{\max} = 22$ for (a) and $\ell_{\max} = 30$ for (b). Since both (a) and (b) have $L < \ell_{\max}$, both modes are in the dynamical localization regime. Though the error bars in Fig. 3 are small enough to make the appreciable fluctuations significant, exponential localization is readily apparent.

Fig. 4 shows data obtained from our measurements of eight modes in the range 5–8.5 GHz where we investigated the dynamical localization regime. The data are plotted versus scaled angular momentum $(\ell - \ell_0)/L$ so that each mode has, in a statistical sense, the same exponential decay. A weighted least-squares fit to all these data gave the solid line, whose slope 0.89 ± 0.19 agrees with the expected slope of 1. Figs. 3 and 4 provide the first experimental confirmation of the predicted existence of exponentially localized modes in rough billiards.

Now we compare our experimental results with finer details of localization theory. Since one expects a wavefunction to be localized near ℓ_r , we use $\ell_r = \ell_0$ for the following analysis of our data. With values of ℓ_0 and L extracted from Fig. 3 and the known values of ℓ_{\max} , we used Eq. (9) to compute

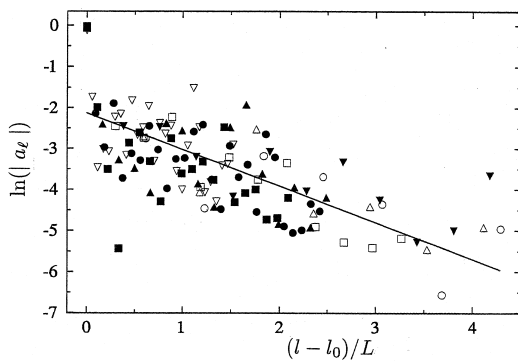


Fig. 4. The angular momentum content of eight exponentially localized modes in the dynamical localization regime 5 GHz $< f < 8.5$ GHz, plotted versus scaled angular momentum $(\ell - \ell_0)/L$. A different symbol is used for each mode. The solid line is a weighted linear, least-squares fit to all data shown.

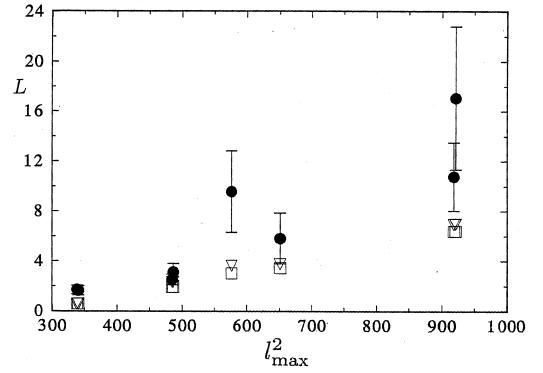


Fig. 5. Comparison between experimental (filled circles) and theoretical (open squares and triangles) localization lengths L . Squares: Direct estimate of L using Eq. (8). Triangles: L computed using Eq. (9).

$\tilde{\kappa}_{\text{eff}}^2$ for each of the two modes, (a) and (b), in Figs. 2 and 3. We obtain $\tilde{\kappa}_{\text{eff};\text{expt}}^2 \approx 0.0023$ and 0.003 , respectively. We may compare these to the theoretical values of the effective roughness according to Eq. (7). Since $\tilde{\kappa}_{\text{eff}}$ exhibits large fluctuations as a function of the cutoff ℓ_{\max} , we averaged the effective roughness over the range $[\ell_{\max} - 2, \ell_{\max} + 2]$ and obtained $\tilde{\kappa}_{\text{eff};\text{theo}}^2 = 0.0015$ and 0.002 , respectively. Thus, respective values of $\tilde{\kappa}_{\text{eff};\text{theo}}^2$ and $\tilde{\kappa}_{\text{eff};\text{expt}}^2$ agree within a factor of two. Using the 753 data points (R_j, θ_j) and linear interpolation between them, we obtain a ‘bare’ cavity roughness $\tilde{\kappa}^2 \approx 0.05$ at a resolution of $\Delta\theta \approx 2\pi/753$. We are not surprised that this roughness is much larger than $\tilde{\kappa}_{\text{eff};\text{theo}}^2$ or $\tilde{\kappa}_{\text{eff};\text{expt}}^2$ because at $\lambda \approx 4$ cm the resolving power of the modes (a) and (b) is much less than the resolution assumed in computing $\tilde{\kappa}^2$.

Fig. 5 compares experimental and theoretical localization lengths computed from Eqs. (8) and (9). The classical diffusion constant D was obtained from numerical trajectory calculations. As shown in Fig. 5, the theoretical localization lengths obtained with the two methods agree. That our experimental data are higher is consistent with the shift observed in Figs. 4 and 5 of Ref. [10].

In summary, we provided the first experimental demonstration of exponential localization in rough billiards. Defining the new concept of effective roughness, we showed that theoretical and experimental roughness parameters are in good agreement

with each other. Theoretically computed localization lengths based on the concept of effective roughness are in good agreement with the experimental results.

Acknowledgements

Sz.B., Y.H., and L.S. acknowledge partial support by KBN grant No. 2 P03B 023 17; P.M.K. by NSF grant PHY-9732443 and R.B. by NSF grant PHY-9900730. We thank the DFG (SFB 185) [NSF, KBN] for supporting this work and providing financial support for L.S.'s visits to Marburg [Stony Brook, Freiburg].

References

- [1] P.W. Anderson, Phys. Rev. 109 (1958) 1492.
- [2] A. Kudrolli, V. Kidambi, S. Sridhar, Phys. Rev. Lett. 75 (1995) 822.
- [3] S.L. McCall, P.M. Platzman, Phys. Rev. Lett. 67 (1991) 2017.
- [4] A.Z. Genack, N. Garcia, Phys. Rev. Lett. 66 (1991) 2064.
- [5] G. Casati, B.V. Chirikov, J. Ford, F.M. Izrailev, in: Stochastic Behavior in Classical and Quantum Hamiltonian Systems, Lecture Notes in Physics, vol. 93, Springer, Berlin, 1979, p. 334.
- [6] S. Fishman, D.R. Grempel, R.E. Prange, Phys. Rev. Lett. 49 (1982) 509.
- [7] D.L. Shepelyansky, Phys. Rev. Lett. 56 (1986) 677.
- [8] G. Casati, B.V. Chirikov, I. Guarneri, D.L. Shepelyansky, Phys. Rep. 154 (1987) 77.
- [9] F. Borgonovi, G. Casati, B. Li, Phys. Rev. Lett. 77 (1996) 4744.
- [10] K.M. Frahm, D.L. Shepelyansky, Phys. Rev. Lett. 78 (1997) 1440.
- [11] K.M. Frahm, D.L. Shepelyansky, Phys. Rev. Lett. 79 (1997) 1833.
- [12] Y. Yamamoto, R.E. Slusher, Phys. Today 46 (1993) 66.
- [13] J.U. Nöckel, A.D. Stone, Nature 385 (1997) 45.
- [14] Ya.M. Blanter, A.D. Mirlin, B.A. Muzykantskii, Phys. Rev. Lett. 80 (1998) 4161.
- [15] F. Borgonovi, Phys. Rev. Lett. 80 (1998) 4653.
- [16] M.V. Berry, in: W. Guttinger, H. Elkeimer (Eds.), Structural Stability in Physics, Springer, Berlin, 1979, pp. 51–53.
- [17] S. Russ, B. Sapoval, O. Haeberlé, Phys. Rev. E 55 (1997) 1413.
- [18] H.-J. Stöckmann, J. Stein, Phys. Rev. Lett. 64 (1990) 2215.
- [19] J. Stein, H.-J. Stöckmann, U. Stoffregen, Phys. Rev. Lett. 75 (1995) 53.